Journal of Naval Science and Engineering
2014, Vol.10, No.1, pp.45-64

AN APPLICATION OF INVESTIGATION ON PREDICTION OF SMOKE PRODUCTION IN A TUNNEL FIRE BY USING A COMPUTER SIMULATION

Erinç DOBRUCALI

Department of Marine Architecture and Marine Engineering
Turkish Naval Academy
edobrucali@yahoo.com

Abstract

Computational fluid dynamics (CFD) is nowadays widely used to simulate smoke spread and temperature distribution as well as ventilation measures in a fire scenario. It allows improving fire fighting strategies and precaution measures in order to suppress the fire as fast as possible and help people to evacuate. In recent years, it has become apparent that computational fluid dynamics (CFD) can play an important and useful role in fire safety problems. The application of CFD to fire problems is also known as field modeling. Field modeling is based on the fundamental laws which govern the fire phenomena. Therefore, it is a valuable alternative for experimental investigations and empirical correlations and can be applied as a predictive tool. In this paper, field modeling is applied to tunnel fires in order to predict the critical ventilation velocity.

BİR TÜNEL YANGININDA DUMAN OLUŞUMUNUN BİLGİSAYAR SİMÜLASYONU KULLANILARAK İNCELENMESİ ÜZERİNE BİR UYGULAMA

Özetçe

Bir yangın senaryosunda havalandırma ayarlamaları, duman yayılımının ve sıcaklık dağılımının simüle edilmesi için hesaplamalı akışkanlar dinamiği (CFD) bugünlerde çok sıkça kullanılmaktadır. Bu yöntem mümkün olduğu kadar hızlı bir şekilde yangını söndürmek ve insanların o bölgeyi boşaltmalarına yardımcı olmak için yangınla mücadele stratejilerinin geliştirilmesi ve önlem ayarlamalarını sağlar. Son yıllarda CFD'nin yangın güvenliği problemlerinde kullanışlı ve önemli bir rol oynadığı açıkça görülmektedir. Yangın problemlerinde CFD uygulaması aynı zamanda saha modellemesi olarak da bilinir.

Saha modellemesi yangın olayını yöneten temel kanunlara bağlıdır. Bu nedenle deneysel araştırmalar ve ampirik korelasyonlar için değerli bir alternatiftir ve öngörülerde bulunmaya yardımcı olan bir araç olarak başvurulabilir. Bu çalışmada tünel yangınlarında kritik havalandırma hızının tespit edilmesi maksadıyla saha modellemesine başvurulmuştur.

Keywords: *Fire, CFD, Field modeling, Tunnel Fire.*
Anahtar Sözcükler: *Yangın, CFD, Saha modellemesi, Tünel yangınları.*

1. MATHEMATICAL MODEL

The **finite-difference technique** is used to discretize the partial differential equations. This procedure entails the subdividing of the calculation domain in to a finite number of cells. The velocities (u_i) are taken on the boundary of each cell ; and all the scalar variables are taken at cell centers. This staggered grid leads to a very efficient differencing scheme for the equations. All spatial derivatives are approximated by second-order central differences and the flow variables are up dated using an explicit **second-order Runge–Kutta scheme**.

The momentum equation is simplified by subtracting off the hydrostatic pressure gradient from the momentum equation, and then dividing by the density. An elliptic partial differential equation can be obtained by taking the divergence of the momentum equations, yielding a Poisson (pressure-like) equation which is solved with a fast, direct method. The inert solid surface is considered as adiabatic, and the no- slip condition is imposed by setting all velocities to zero. The burning surface is considered as a pure combustible material.

At the tunnel entrance, an open boundary condition is used, allowing combustion products to exit through the entrance if the backflow is sufficiently strong. The pressure is prescribed depending on whether the flow is incoming or outgoing at the tunnel entrance.

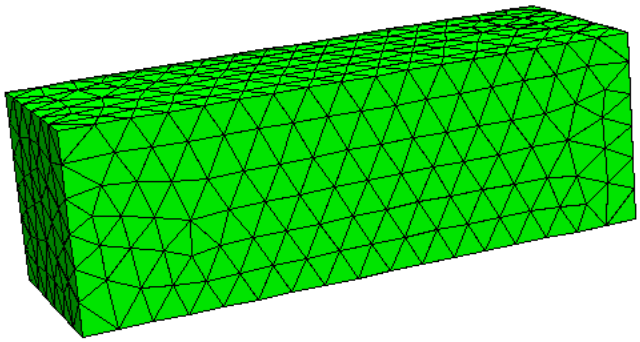

Figure: 1.1. Meshed rectangular prism

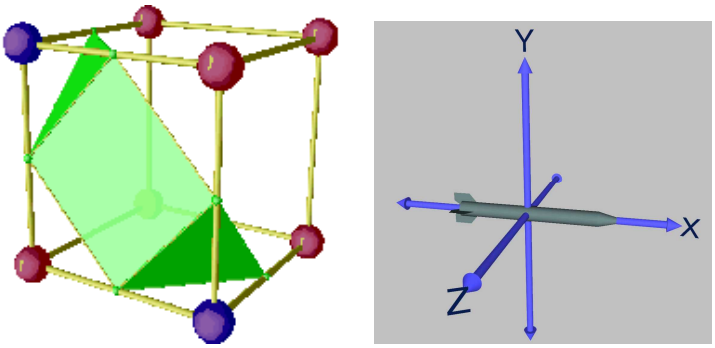

Figure: 1.2. One example cubic volume of meshed cubic volume

The finite-difference:

For example: $\frac{\partial \rho}{\partial t} + \frac{\partial (\rho . u_j)}{\partial x_j} = 0$

$$\downarrow \qquad \downarrow$$

$$\frac{\rho_{1,t1} - \rho_{2,t2}}{t_1 - t_2}$$

3D : x: $\frac{\partial(\rho u)}{\partial(x)} = \frac{(\rho u)_2 - (\rho u)_1}{x_2 - x_1}$

y: $\frac{\partial(\rho v)}{\partial(y)} = \frac{(\rho v)_7 - (\rho v)_1}{y_7 - y_1}$

z: $\frac{\partial(\rho w)}{\partial(z)} = \frac{(\rho w)_3 - (\rho w)_1}{z_3 - z_1}$

Second Order Runge-Kutta:

$k_1 = h.f(x_n , y_n)$ h:Step size

$k_2 = h.f(x_n + \frac{1}{2} h, y_n + \frac{1}{2} k_1)$

$y_{n+1} = y_n + k_2 + O(h^2)$

These partial differential equations which are selected in this study are solved by FLUENT 6.3 simulation program.

CONTİNUITY AND MOMENTUM EQUATIONS: For all flows, **FLUENT** solves conservation equations for mass and momentum. For flows involving heat transfer or compressibility, an additional equation for energy conservation is solved. For flows involving species mixing or reactions, a species conservation equation is solved or, if the non-premixed combustion model is used, conservation equations for the mixture fraction and its

variance are solved. Additional transport equations are also solved when the flow is turbulent.

RADIATIVE TRANSFER EQUATION: The DTRM and the P-1, Rosseland, and DO radiation models require the absorption coefficient a as input. a and the scattering coefficient σ_s can be constants, and a can also be a function of local concentrations of H_2O and CO_2, path length, and total pressure. **FLUENT** provides the weighted-sum-of-gray-gases model (WSGGM) for computation of a variable absorption coefficient. The discrete ordinates implementation can model radiation in semi-transparent media. The refractive index n of the medium must be provided as a part of the calculation for this type of problem. The Rosseland model also requires you to enter a refractive index, or use the default value of 1.

MODELING SPECIES TRANSPORT AND FINITE-RATE CHEMISTRY: **FLUENT** can model the mixing and transport of chemical species by solving conservation equations describing convection, diffusion, and reaction sources for each component species. Multiple simultaneous chemical reactions can be modeled, with reactions occurring in the bulk phase (volumetric reactions) and/or on wall or particle surfaces, and in the porous region.

SOOT FORMATION: **FLUENT** provides two empirical models for the prediction of soot formation in combustion systems. In addition, the predicted soot concentration can be included in the prediction of radiation absorption coefficients within the combustion system. We can include the effect of soot on radiation absorption when we use the P-1, discrete ordinates, or discrete transfer radiation model with a variable absorption coefficient.

2. SOLUTION

The finite-difference technique is used to discretize the *partial differential* equations. This procedure entails the subdividing of the calculation domain into a finite number of cells. The velocities (u_i) are taken

on the boundary of each cell; and all the scalar variables are taken at cell centres.This staggered grid leads to a very efficient differencing scheme for the equations. All spatial derivatives are approximated by second-order central differences and the flow variables are updated using an explicit **second-order Runge–Kutta scheme**.

But it is studied 2 dimensional (2D) Modeling Species Transport and Gaseous Combustion tutorial after 5.1.3 Programs solution steps part.

2.1 Parameters

2.1.1 Physical Properties

ρ = Density (It changes with time[t] an x, y, z direction variables)
g_i = Acceleration of gravity in the co-ordinate directions x, y and z
μ_t = Turbulent viscosity
T = Temperature
P= Pressure

2.1.2. Physical Constants

C_s= Smagorinsky constant **= *0.21***
C_μ, C_e empirical constants in turbulence model ***=0.0856, 0.845***
f–g =constant in soot model
α, β = constants in soot model
σ =Stefan–Boltzmann constant
κ =total absorption coefficient
A_0= Constant in soot model
C_{EBU} = Constant in EBU model

2.2. Programs solution steps

2.2.1 Grid step

$\mathbf{X_{max}}$ and $\mathbf{Y_{max}}$ are 90 and 2.4 m, respectively. I changed Scale factors X=50 and Y= 10.66. There is a rectangular prism model meshed like the Figure 5.1

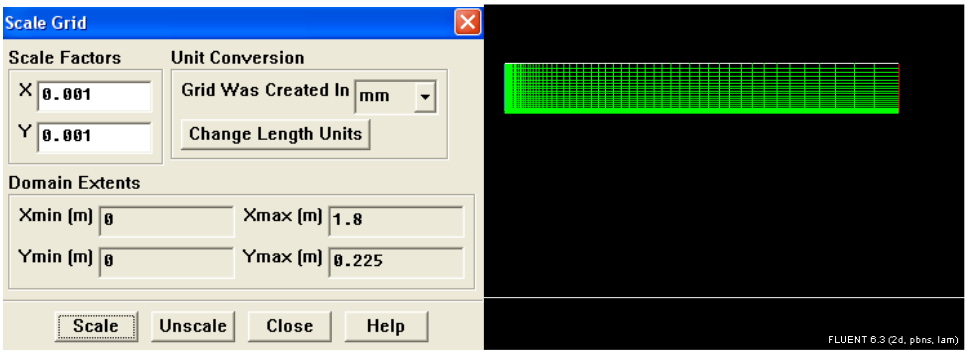

Figure 2.1. Grid scale

2.2.2. Models Step

After it is composed a grid scale, it can be change the models in FLUENT. It will defined the domain as axisymmetric for solver.

It will be enable heat transfer by enabling the energy equation and select the standard k- ϵ (2-equation) turbulence model for viscous

It will be enable chemical species transport and reaction. Mixture properties is selected n-*octane air* for my model. Turbulance-chemistry interaction is selected *Eddy-Dissipation* and reactions is selected *volumetric*. The eddy-dissipation model computes the rate of reaction under the assumption that chemical kinetics are fast compared to the rate at which reactants are mixed by turbulent fluctuations (eddies).

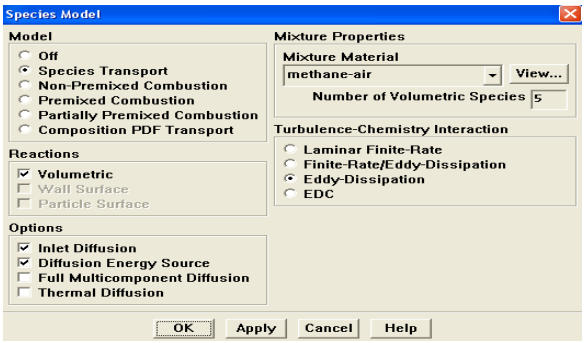

2.2.3. Materials Step

In this model, mixture is n-octane air and selected species are **C_8H_{18}, O_2, CO_2, H_2O, N_2**.

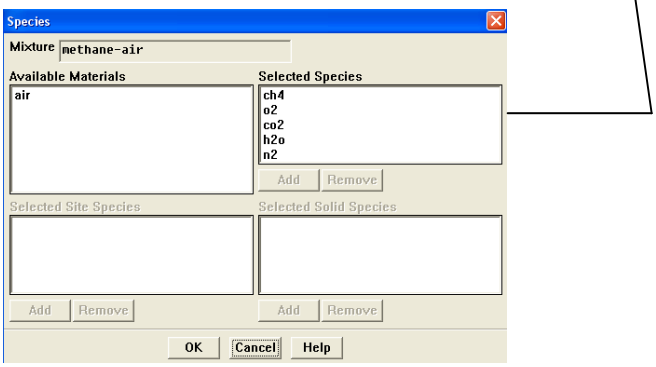

In this model, mixture part is octane-air and coefficients are different. The eddy-dissipation reaction model ignores chemical kinetics (i.e., the Arrhenius rate) and uses only the parameters in the Mixing Rate group box in the Reactions panel. The Arrhenius Rate group box is therefore inactive. (The values for Rate Exponent and Arrhenius Rate parameters are included in the database and are employed when the alternate finite-rate/eddy-dissipation model is used.)

For material box, C_p is constant 1000 J/kg-K . The initial calculation will be performed assuming that all properties except density are constant. The use of constant transport properties (viscosity, thermal conductivity, and mass diffusivity coefficients) is acceptable because the flow is fully turbulent. The molecular transport properties will play a minor role compared to turbulent transport. The assumption of constant specific heat, however, has a strong effect on the combustion solution.

2.2.4. Boundary Conditions

It will be converted the symmetry zone to the axis type. The symmetry zone must be converted to an axis to prevent numerical difficulties where the radius reduces to zero.

It will be entered `air-inlet` for **Zone Name.** Velocity is 0.5 m/s, hydraulic height of this tunnel is 3.3 m.

It will be entered `fuel-inlet` for **Zone Name.** Hydraulic Diameter is for fire is 1.2m. The **Backflow** values in the **Pressure Outlet** panel are utilized only when backflow occurs at the pressure outlet. Reasonable values should always be assigned, since backflow may occur during intermediate iterations and could affect the solution stability.

It will be set the boundary conditions for the outer wall (**wall-7**). And set the boundary conditions for the fuel inlet nozzle (**wall-2**).

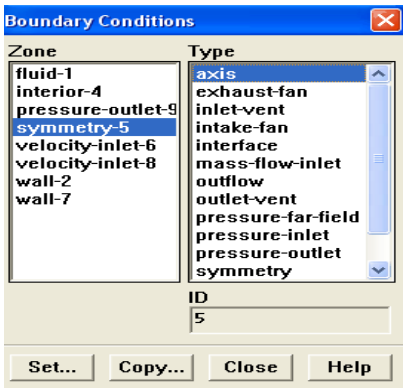

2.2.5. Initial Solution with Constant Heat Capacity

I will be entered `0.95` for each of the species (**C_8H_{18}**, **O_2**, **CO_2**, and **H_2O**) in the **Under-Relaxation Factors** group box.

The default under-relaxation parameters in **FLUENT** are set to high values. For a combustion model, it may be necessary to reduce the under-relaxation to stabilize the solution. Some experimentation is typically necessary to establish the optimal under-relaxation. For this tutorial, it is sufficient to reduce the species under-relaxation to 0.95. The solution will converge in approximately 300 iterations

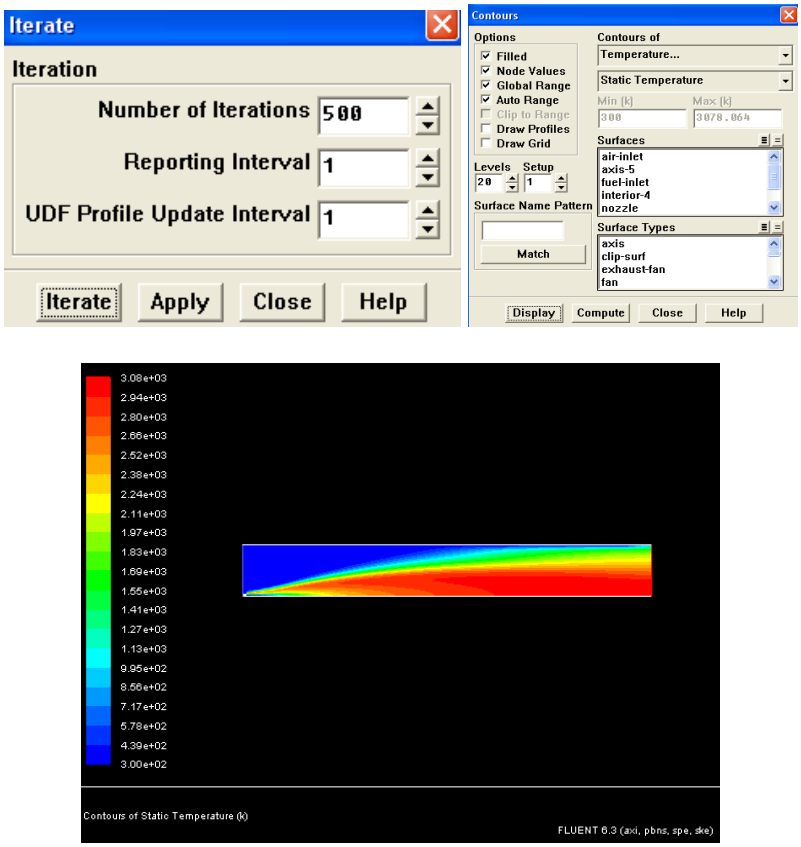

Figure 2.2. Static Temperature

The peak temperature, predicted using a constant heat capacity of 1000 J/kg-K, is over 3000 K. This over prediction of the flame temperature can be remedied by a more realistic model for the temperature and

composition dependence of the heat capacity, as illustrated in the next step of the tutorial.

2.2.6. Solution with Varying Heat Capacity Step

The strong temperature and composition dependence of the specific heat has a significant impact on the predicted flame temperature. In this step, it will be used the temperature-varying property information in the **FLUENT** database to recompute the solution.

It is selected **mixing-law** from the **Cp** drop-down list in the **Properties** group box. The specific heat of the mixture will now be based on a local mass-fraction-weighted average of all the species.

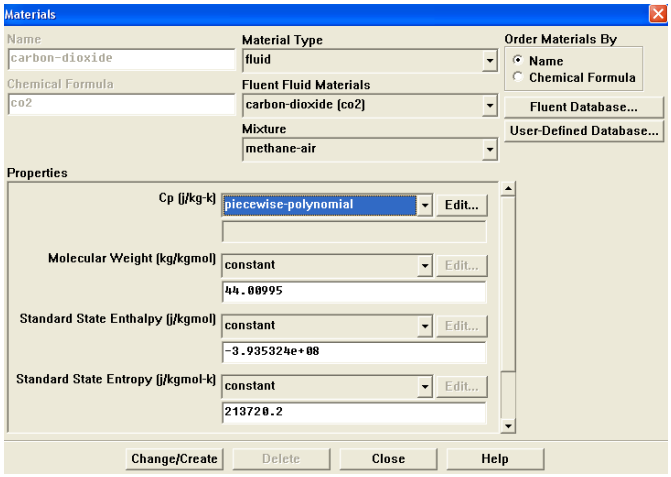

It is selected **carbon-dioxide (CO_2)** from the **Fluent Fluid Materials** drop-down list and **piecewise-polynomial** from the **Cp** drop-down list in the **Properties** group box. In a similar manner, enable temperature dependence of specific heat for the remaining species (C_8H_{18}, N_2, O, and H O).

And now, it is requested 500 more iterations. The residuals will jump significantly as the solution adjusts to the new specific heat representation. The solution will converge after approximately 230 additional iterations.

3. POSTPROCESSING

Lets review the solution by examining graphical displays of the results and performing surface integrations at the combustor exit. The peak temperature has dropped to approximately 2300 K as a result of the temperature and composition-dependent specific heat. Temperature distribution displays in Figure 6.1. Spesific heat displays in Figure 6.2

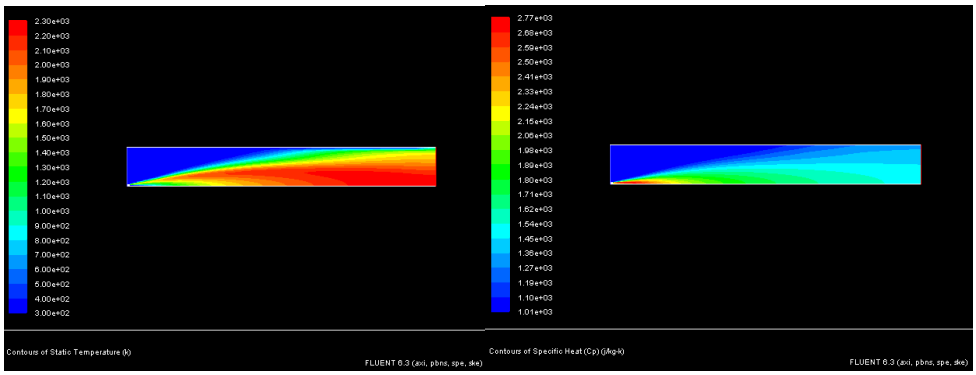

Figure 3.1. Contours of Temperature **Figure 3.2**. Contours of Spesific Heat variables C_p

The mixture specific heat is largest where the C_8H_{18} is concentrated, near the fuel inlet, and where the temperature and combustion product concentrations are large. The increase in heat capacity, relative to the constant value used before, substantially lowers the peak flame temperature.

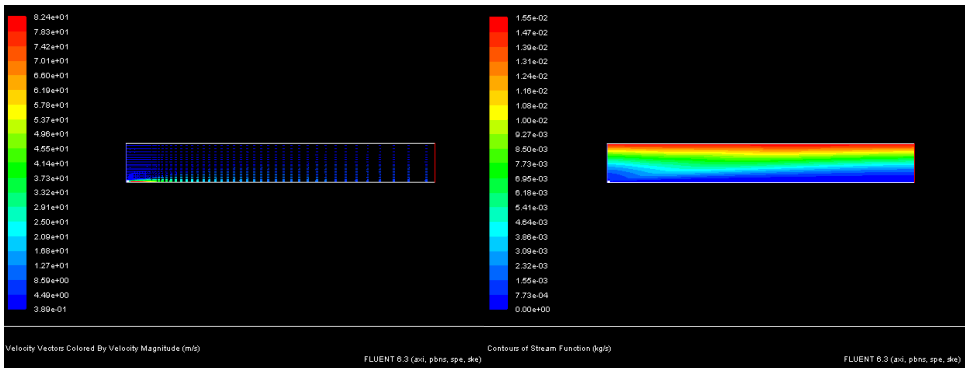

Figure 3.3. Velocity vectors **Figure 3.4.** Contours of Stream Function

The entrainment of air into the high-velocity methane jet is clearly visible in the streamline display. Lets display filled contours of mass fraction for C_8H_{18} and O_2, CO_2, and H_2O respectively.

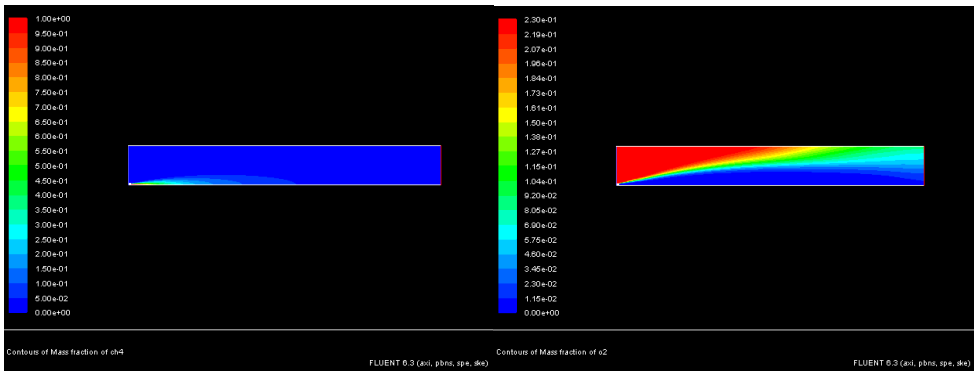

Figure 3.5. Mass Fraction C_8H_{18} **Figure 3.6.** Mass Fraction O_2

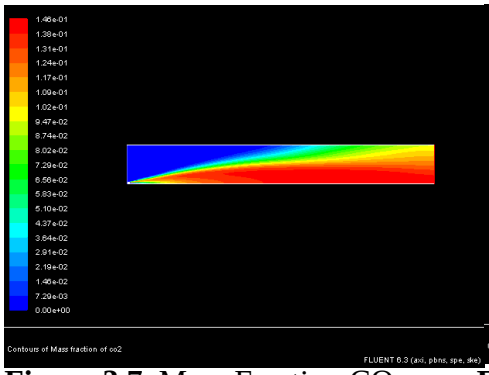

Figure 3.7. Mass Fraction CO_2

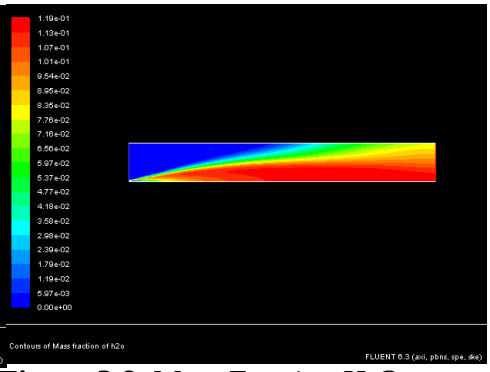

Figure 3.8. Mass Fraction H_2O

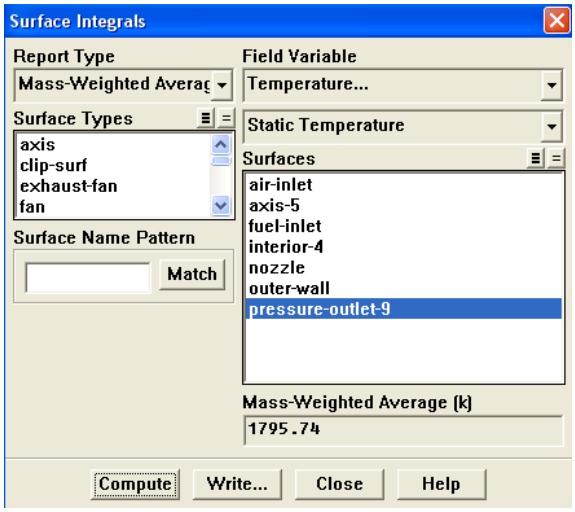

The mass-averaged temperature will be computed as:

$$\overline{T} = \frac{\int T\rho\vec{v}\cdot d\vec{A}}{\int \rho\vec{v}\cdot d\vec{A}}$$

The **Mass-Weighted Average** field will show that the exit temperature is approximately 1796 K.

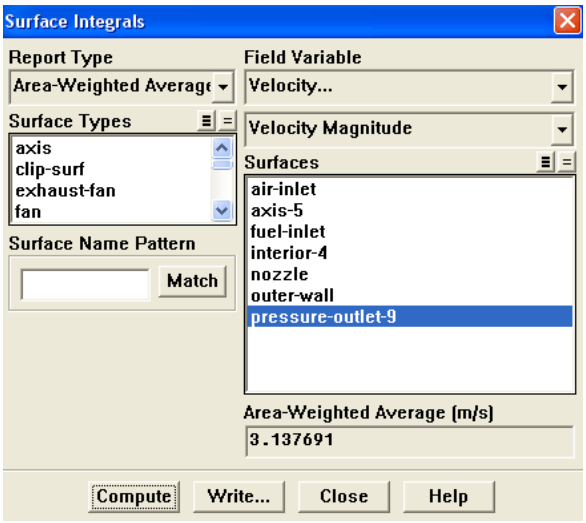

The area-weighted velocity-magnitude average will be computed as:

$$\bar{v} = \frac{1}{A}\int v\, dA$$

The **Area-Weighted Average** field will show that the exit velocity is approximately 3.14 m/s.

3.1 NOx Prediction Step

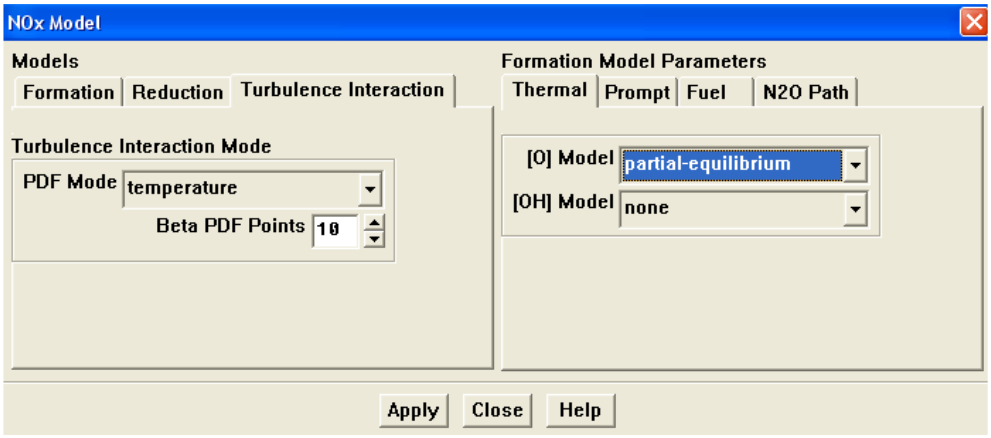

This will be enable the turbulence-chemistry interaction. If turbulence interaction is not enabled, you will be computing NOx formation without considering the important influence of turbulent fluctuations on the time-averaged reaction rates.

It will be predicted NO_X formation in a "postprocessing" mode, with the flow field, temperature, and hydrocarbon combustion species concentrations fixed. Thus, only the NO equation will be computed. Prediction of NO in this mode is justified on the grounds that the NO concentrations are very low and have negligible impact on the hydrocarbon combustion prediction. And now it has to be iterated 50 more times. It converges immediately.

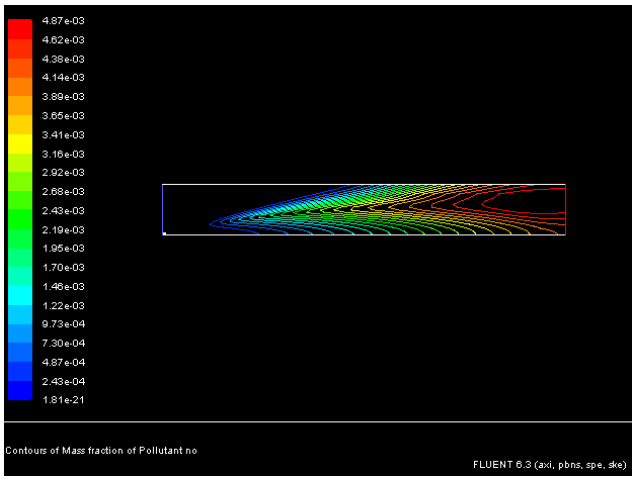

Figure 3.9. Contours of NO Mass Fraction

The peak concentration of NO is located in a region of high temperature where oxygen and nitrogen are available. It will be calculated the average exit NO mass fraction now. The **Mass-Weighted Average** field will show that the exit NO mass fraction is approximately 0.00464. Now it will be iterated 50 more times.

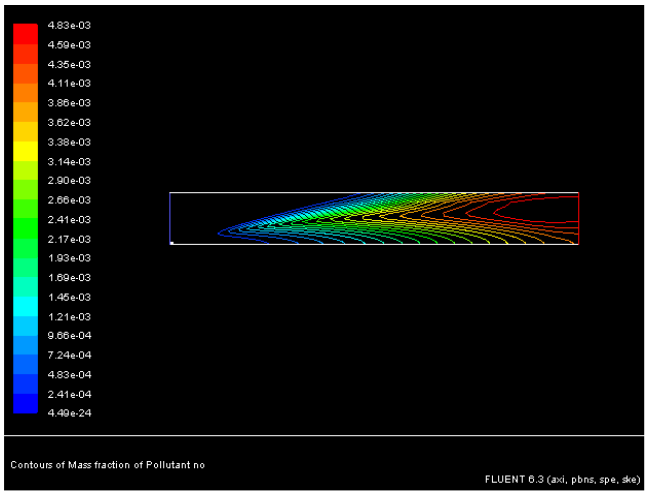

Figure 4. Contours of NO mass fraction: Thermal NO_x formation

The concentration of NO is slightly lower without the prompt NOx mechanism. Now it will be used a custom field function to compute NO parts per million (ppm). NO ppm will be computed from the following equation:

$$\text{NO ppm} = \frac{\text{NO mole fraction} \times 10^6}{1 - \text{H}_2\text{O mole fraction}}$$

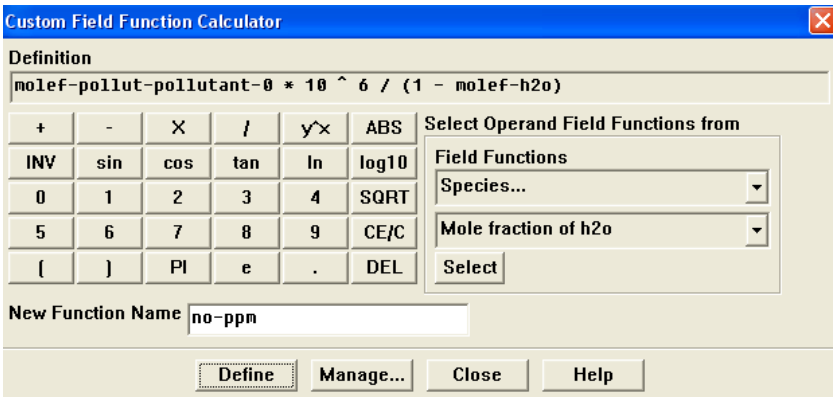

4. SUMMARY AND CONCLUSION

The procedures used here for simulation of hydrocarbon combustion can be applied to other reacting flow systems. This exercise illustrated the important role of the mixture heat capacity in the prediction of flame temperature. The combustion modeling results are summarized in the following table.

	Peak Temp.	Exit Temp.	Exit Velocity
	(K)	(K)	m/s
Constant C_p	3078	2198	3.84
Variable C_p	2302	1796	3.14

The use of a constant C_p results in a significant over prediction of the peak temperature. The average exit temperature and velocity are also over predicted.

The variable C_p solution produces dramatic improvements in the predicted results. Further improvements are possible by considering additional models and features available in **FLUENT**.

The NO_X production in this case was dominated by the thermal NO mechanism. This mechanism is very sensitive to temperature. Every effort should be made to ensure that the temperature solution is not over predicted, since this will lead to unrealistically high predicted levels of NO.

REFERENCES

[1] Kevin B. McGrattan, Anthony Hamins, 2001, Numerical Simulation of the Howard Street Tunnel Fire, Fire Research Division Building and Fire Research Laboratory.

[2] A.R.Nilsen, T.Log, 2009, Results from three models compared to full-scale tunnel fires tests Fire Safety Journal 44 (2009) 33– 49.

[3] J. Collazo, J. Porteiro *, D. Patiño, J.L. Miguez, E. Granada, J. Moran, 2009, Simulation and experimental validation of a methanol burner, Fuel 88 (2009) 326–334.

[4] I.S. Lowndesa, S.A. Silvestera,, D. Giddingsb, S. Pickeringb, A. Hassanb, E. Lester, 2007, The computational modelling of flame spread along a conveyor belt, Fire Safety Journal 42 (2007) 51–67.
[5] F. Liu, J.X. Wen, 2002, The effect of turbulence modelling on the CFD simulation of buoyant diffusion flames, Fire Safety Journal 37 (2002) 125–150.
[6] D. Rusch, L. Blum, A. Moser, T. Roesgen, 2008, Turbulence model validation for fire simulation by CFD and experimental investigation of a hot jet in crossflow, Fire Safety Journal 43 (2008) 429–441.
[7] J.P. Kunsch, 2002, Simple model for control of fire gases in a ventilated tunnel, Fire Safety Journal 37 (2002) 67–81.
[8] C.C. Hwang_, J.C. Edwards, 2005, The critical ventilation velocity in tunnel fires—a computer simulation, Fire Safety Journal 40 (2005) 213–244.
[9] Y. Wu, M.Z.A. Bakar, 2000, Control of smoke Flow in tunnel fires using longitudinal ventilation systems a study of the critical velocity, Fire Safety Journal 35 (2000) 363}390.
[10] Sherman C.P. Cheunga, Richard K.K. Yuena,, G.H. Yeohb, Grace W.Y. Cheng, 2004, Contribution of soot particles on global radiative heat transfer in a two-compartment fire, Fire Safety Journal 39 (2004) 412–428.
[11] Karim Van Maele, Bart Merci, 2008, Application of RANS and LES field simulations to predict the critical ventilation velocity in longitudinally ventilated horizontal tunnels, Fire Safety Journal 43 (2008) 598–609.